Figure 12: CRE Debt and Equity Ownership

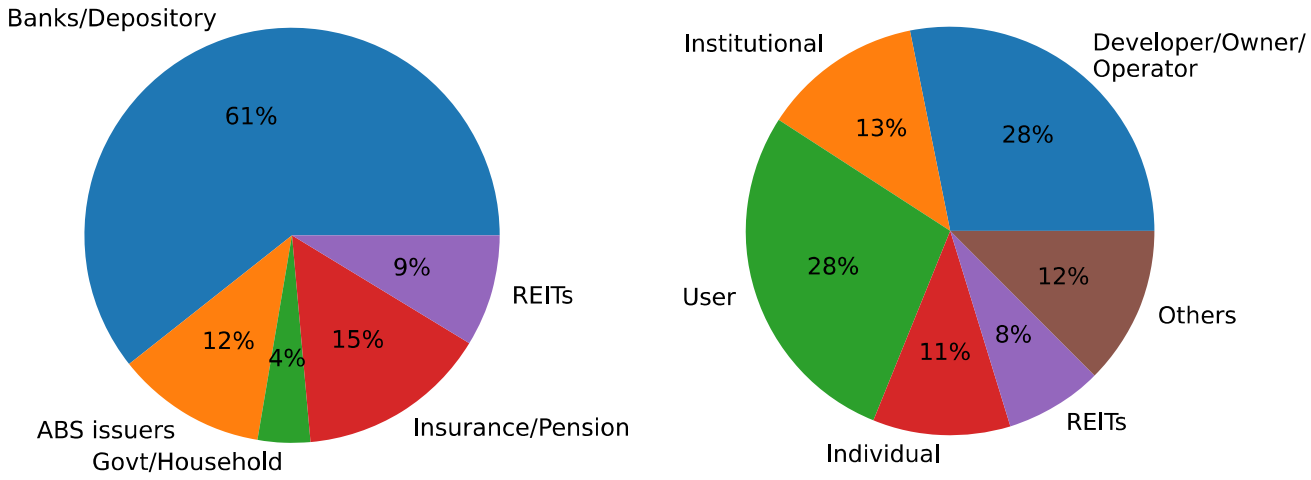

Panel A: Debt Ownership (All CRE, 2022)

Panel B: Equity Ownership (Office, 2020)

Notes: Debt ownership data is from the Federal Reserve Flow of Funds data and office ownership is from Real Capital Analytics.

Figure 13: Commercial Real Estate By Bank Size

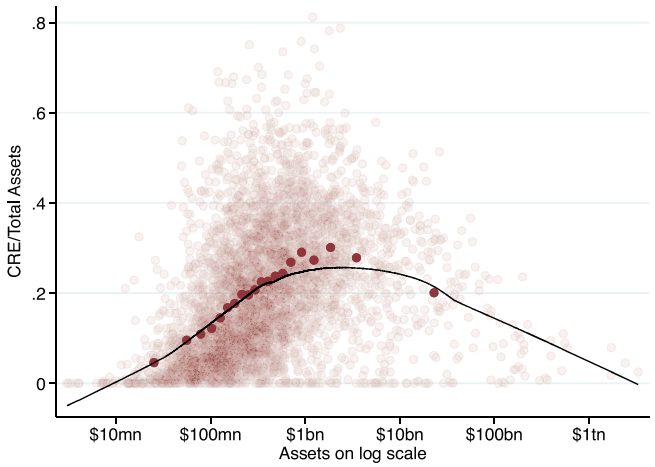

Notes: Data are from 2020.Q4 Bank Call Reports.

Figure 14: Repercussions of Commercial Real Estate Valuation on Governments

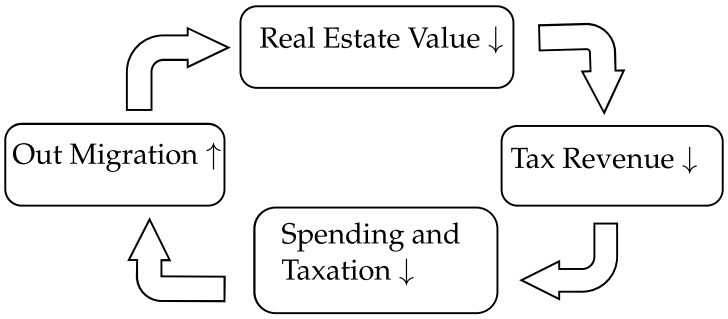

have been hit as hard as office, has important implications for local public finances. For example, the share of property taxes in NYC's budget was 48% in 2021, 31% of which comes from office and retail property taxes.[25] A 49.2% decline in property values would, over time, result in a 7.3% reduction in overall tax revenues. Given budget balance requirements, the fiscal hole left by declining commercial property tax revenues would need to be plugged by either raising other tax rates or cutting government spending (public safety, transit, sanitation, education, etc.). Both would reduce the attractiveness of the city as a place of residence and work, and result in increased out-migration. These dynamics risk activating an "urban doom loop" (Figure 14) of lower tax revenues, reduced government services, and population loss. With more people being able to separate the location of work and home, the migration elasticity to local tax rates and amenities may now be larger than in the past. Future research should explore these implications and study the role for local and federal policy to mitigate the urban doom loop.

Trends in office occupancy have prompted discussion on the merits of conversion of office, either from A-/B/C to A+ office or to alternative use such as residential. The former conversion could make sense in light of the flight to quality and the likely dearth of new office construction for years to come. The latter conversion makes sense in light of the lack of (affordable) housing in large cities, but often runs into issues relating to the structural feasibility, zoning restrictions, and return on investment (Gupta et al., 2023). Older buildings tend to be more amenable to apartment conversion. Whether and how these conversions take place will have an important impact on the vibrancy of neighborhoods and the future of cities. Given the negative externalities associated with office vacancy, there is a role for local governments to facilitate conversions and speed up the transition towards a smaller office stock and larger housing stock.

[25] An additional 3% of tax revenue comes from a tax on real estate tenants, and there are further indirect effects on sales and income tax from weakness in downtown office and retail. Office property tax collection alone exceeds the combined budgets of Sanitation, Fire, Transportation, and Parks and Recreation departments in NYC.

References

Aksoy, Cevat Giray, Jose Maria Barrero, Nicholas Bloom, Steven J. Davis, Mathias Dolls, and Pablo Zárate, "Working From Home Around the World," *BPEA Conference Draft*, 2022.

Badarinza, Cristian, Tarun Ramadorai, and Chihiro Shimizu, "Gravity, counterparties, and foreign investment," *Journal of Financial Economics*, 2022, *145* (2), 132–152.

Barnett, Michael, William Brock, and Lars Peter Hansen, "Pricing uncertainty induced by climate change," *The Review of Financial Studies*, 2020, *33* (3), 1024–1066.

Barrero, Jose Maria, Nicholas Bloom, and Steven Davis, "Why Working from Home Will Stick," Working Paper 28731, National Bureau of Economic Research apr 2021.

Barrero, José María, Nicholas Bloom, and Steven J Davis, "The Evolution of Work from Home," *Journal of Economic Perspectives*, 2023, *37* (4), 23–49.

Bartik, Alexander W, Zoe B Cullen, Edward L Glaeser, Michael Luca, and Christopher T Stanton, "What jobs are being done at home during the COVID-19 crisis? Evidence from firm-level surveys," Working Paper 27422, National Bureau of Economic Research 2020.

Benmelech, Efraim, Mark J Garmaise, and Tobias J Moskowitz, "Do liquidation values affect financial contracts? Evidence from commercial loan contracts and zoning regulation," *The Quarterly Journal of Economics*, 2005, *120* (3), 1121–1154.

Bick, Alexander, Adam Blandin, and Karel Mertens, "Work from Home Before and After the COVID-19 Outbreak," *American Economic Journal: Macroeconomics, forthcoming*, 2023.

Bloom, Nicholas, Ruobing Han, and James Liang, "How Hybrid Working From Home Works Out," Working Paper 30292, National Bureau of Economic Research July 2022.

Brueckner, Jan K, Matthew E Kahn, and Gary C Lin, "A new spatial hedonic equilibrium in the emerging work-from-home economy?," *American Economic Journal: Applied Economics*, 2023, *15* (2), 285–319.

Brynjolfsson, Erik, John J Horton, Christos Makridis, Alexandre Mas, Adam Ozimek, Daniel Rock, and Hong-Yi TuYe, "How Many Americans Work Remotely? A Survey of Surveys and Their Measurement Issues," Working Paper 31193, National Bureau of Economic Research 2023.

Cvijanović, Dragana, Stanimira Milcheva, and Alex van de Minne, "Preferences of Institutional Investors in Commercial Real Estate," *The Journal of Real Estate Finance and Economics*, may 2021, *65*, 321–359.

Davis, Morris A, Andra C Ghent, and Jesse M Gregory, "The work-from-home technology boon and its consequences," Working Paper 28461, National Bureau of Economic Research 2021.

Delventhal, Matthew J., Eunjee Kwon, and Andrii Parkhomenko, "JUE Insight: How do cities change when we work from home?," *Journal of Urban Economics*, 2022, *127*, 103331. JUE Insights: COVID-19 and Cities.

Eisfeldt, Andrea L, Gregor Schubert, and Miao Ben Zhang, "Generative AI and Firm Values," *Available at SSRN*, 2023.

Gârleanu, Nicolae, Leonid Kogan, and Stavros Panageas, "Displacement risk and asset returns," *Journal of Financial Economics*, 2012, *105* (3), 491–510.

Geltner, David, "Estimating market values from appraised values without assuming an efficient market," *Journal of Real Estate Research*, 1993, *8* (3), 325–345.

Goetzmann, William N, Christophe Spaenjers, and Stijn Van Nieuwerburgh, "Real and Private-Value Assets," *The Review of Financial Studies*, 04 2021, *34* (8), 3497–3526.

Gokan, Toshitaka, Sergei Kichko, Jesse Matheson, and Jacques-François Thisse, "How the rise of teleworking will reshape labor markets and cities," Working Paper 9952, CESifo 2022.

Gupta, Arpit, Candy Martinez, and Stijn Van Nieuwerburgh, "Converting Brown Offices to Green Apartments," Working Paper 31530, National Bureau of Economic Research August 2023.

_ , Vrinda Mittal, Jonas Peeters, and Stijn Van Nieuwerburgh, "Flattening the curve: Pandemic-Induced revaluation of urban real estate," *Journal of Financial Economics*, nov 2022, *146* (2), 594–636.

Jiang, Erica Xuewei, Gregor Matvos, Tomasz Piskorski, and Amit Seru, "US Bank Fragility to Credit Risk in 2023: Monetary Tightening and Commercial Real Estate Distress," Working Paper 2023.

Kim, Hyunseob and Howard Kung, "The asset redeployability channel: How uncertainty affects corporate investment," *The Review of Financial Studies*, 2017, *30* (1), 245–280.

Kogan, Leonid and Dimitris Papanikolaou, "Growth opportunities, technology shocks, and asset prices," *The Journal of Finance*, 2014, *69* (2), 675–718.

_ and _, "Technological innovation, intangible capital, and asset prices," *Annual Review of Financial Economics*, 2019, *11*, 221–242.

Krainer, John et al., "Natural vacancy rates in commercial real estate markets," *FRBSF Economic Letter*, 2001.

Li, Wenli and Yichen Su, "The great reshuffle: Residential sorting during the covid-19 pandemic and its welfare implications," *Available at SSRN 3997810*, 2021.

Mondragon, John A and Johannes Wieland, "Housing Demand and Remote Work," Working Paper 30041, National Bureau of Economic Research 2022.

Monte, Ferdinando, Charly Porcher, and Esteban Rossi-Hansberg, "Remote Work and City Structure," Technical Report, Working Paper 2023.

Nathaniel, Heblich Stephan Baum-Snow and Stuart Rosenthal, "Filtering in Commercial Real Estate," Working Paper 2022.

Papanikolaou, Dimitris, "Investment shocks and asset prices," *Journal of Political Economy*, 2011, *119* (4), 639–685.

Pástor, L'uboš, Robert F Stambaugh, and Lucian A Taylor, "Dissecting green returns," *Journal of Financial Economics*, 2022, *146* (2), 403–424.

Ramani, Arjun and Nicholas Bloom, "The Donut effect of COVID-19 on cities," Working Paper 28876, National Bureau of Economic Research 2021.

Rosenthal, Stuart S., William C. Strange, and Joaquin A. Urrego, "JUE insight: Are city centers losing their appeal? Commercial real estate, urban spatial structure, and COVID-19," *Journal of Urban Economics*, jul 2021, *127*, 103381.

van Binsbergen, Jules, Michael Brandt, and Ralph Koijen, "On the Timing and Pricing of Dividends," *American Economic Review*, 2012, *102* (4), 1596–1618.

Van Nieuwerburgh, Stijn, "The remote work revolution: Impact on real estate values and the urban environment: 2023 AREUEA Presidential Address," *Real Estate Economics*, 2023, *51* (1), 7–48.

Online Appendix

A Additional Empirical Results

A1 Evolution of Prices and Quantities of Newly-Signed Leases

New Lease Rents We study the dynamics of net effective rents (NER) on newly-signed leases. Figure A1 shows the square-foot weighted average NER on new leases, expressed in December 2022 dollars. Panel A shows results for the U.S. and Panel B subsets on NYC. Nationally, the NER fell by 12.48% in 2020. Starting in early 2021, the NER on newly-signed leases experienced a reversal with the NER ending up back at its pre-pandemic level at the end of our sample (dashed line). In NYC, the NER decline on new leases in 2020 is sharper at 14.20%, and the rebound in 2021 and 2022 is weaker.

Figure A1: Net Effective Rent on New Leases

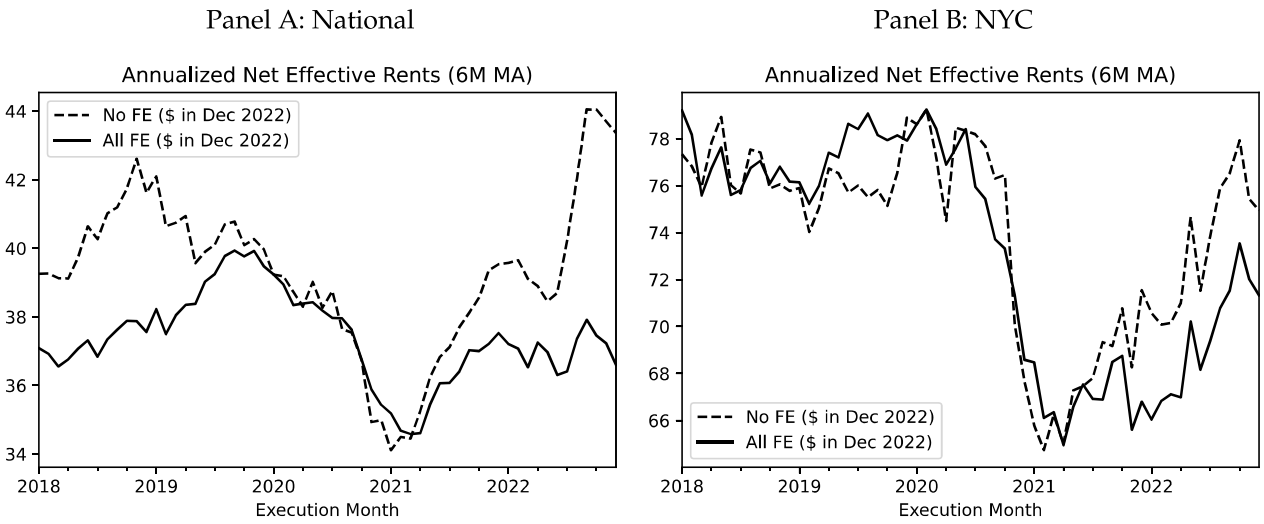

Notes: Panel A shows annualized net effective rents for all markets, while Panel B shows the NER for NYC. Dashed lines denote raw data while solid lines remove tenant industry, renewal, building class, state (panel A), major/non-major market (panel A), and submarket (panel B) fixed effects. Data are sourced from CompStak.

The national average NER dynamics may very well reflect composition effects, either in terms of the markets in which new leases are being signed or in terms of the types of tenants signing new leases. To partially control for such selection effects, we remove tenant-industry and geographical fixed effects. Once fixed effects are removed (solid line), both the decline in NER in 2020 and the rebound in 2021 become weaker. Much of the recent rebound in NER in the raw data turns out to be a spatial composition effect. We recall that this partial rebound happens amidst weak new leasing activity, and likely remaining selection on latent tenant or building quality. The measurement in NYC is less sensitive to the removal of tenant and submarket fixed effects. Again, the NER rebound weakens after fixed effects

are removed.

New Lease Quantities Figure A2 investigates the effect of changes in office demand on the volume of new lease agreements. To do so, we aggregate the total number of new commercial office leases signed in the CompStak data. We observe a large decrease in the quantity of new leases signed, sometimes called absorption, in the left panel of Figure A2. The volume of newly signed leases fell from 290.11 million square feet (sf) per year in the last six months of 2019 to 102.64 million sf per year in the last six months of 2022. The graph suggests a large reduction in office demand from tenants who are actively making space decisions.

Figure A2: Quantity of New Leases Signed

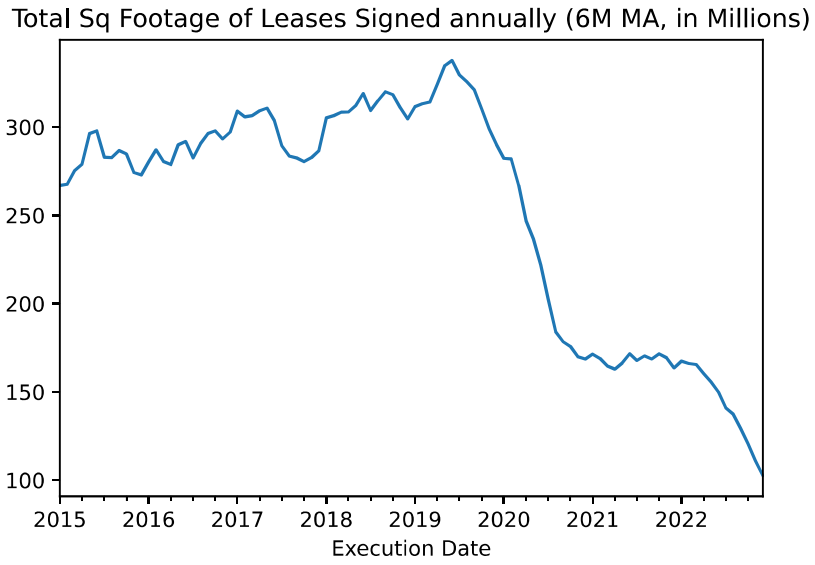

Notes: The graph shows the quantity of leases signed in square feet over time. Data are sourced from CompStak.

New Lease Durations Even when tenants do renew leases, they may not do so under the same set of terms. Panel A of Figure A3 shows that the share of new leases signed that are less than three years in duration increased substantially during the pandemic, while the share of leases with a duration more than seven years decreased meaningfully.

The shortening of lease duration suggests important shifts in the commercial office market, even conditional on lease renewal. As a result, the coming years 2023–2025 will feature even larger than expected lease expiration from two channels: the pre-scheduled expiration of long-term leases signed before the pandemic, as well as the expiration of short-term leases signed during the pandemic. The

distribution of lease maturities as of the end of 2022 is shown in Panel B of Figure A3.

Figure A3: Lease Durations and Current Expiration Schedule

Panel A: Lease Duration Changes

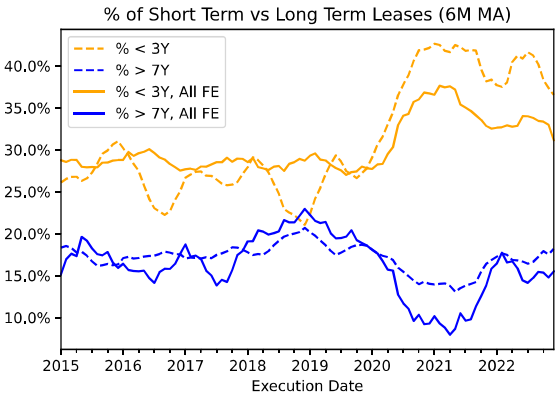

Panel B: 2022 Expiration Schedule

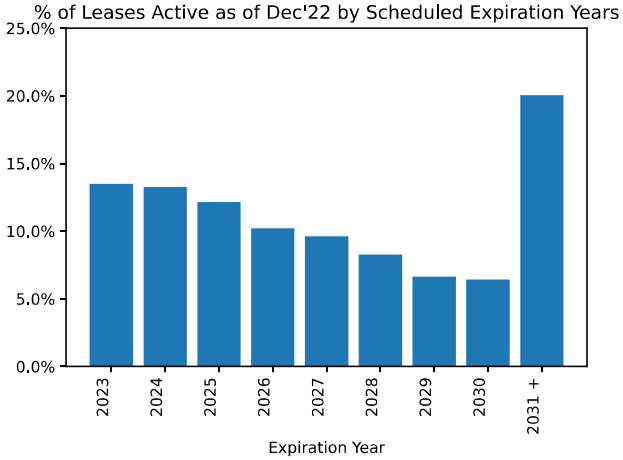

Notes: Panel A shows the share of short-term (less than 3 year duration, in orange) and the share of long-term (more than 7 year duration, in blue) leases over time. Dashed lines denote raw data while the solid lines remove state, major/non-major market, industry, and renewal fixed effects. Panel B shows the percentage of leases expiring per year in square feet for leases that were in force as of December 2022. Data are sourced from CompStak.

A2 Flight To Quality

We label the highest quality buildings as class A+ properties, defined based on rent levels. Specifically, we isolate leases that are in the top ten percent of the NER distribution in each quarter and submarket among all properties that are ranked as Class A by CompStak. We categorize a building that has such a lease as A+ and assume that the A+ status remains for ten years, unless another top-10% lease is signed in that building at which point the ten-year clock resets. By this definition, 34.0% of square feet and 41.0% of lease revenue is in A+ office buildings in New York City. The remaining buildings ("others") are classes "A-" (A without A+), B, and C.

Figure A4 shows net effective rents (NER) on newly-signed leases grouped by building class. We focus on the solid lines, which remove fixed effects. Nationally, A+ rents on new leases show resilience, rising modestly between December 2019 and December 2022. Lower-quality office rents, by contrast, see a decline over this period. The same patterns are present in NYC, shown in Panel B.

Figure A5 considers an alternative building quality measure based on building age. Younger buildings are defined as those constructed in or after 2010. Panel A displays changes in NER per square foot on *newly-signed* leases in NYC. Properties defined as A+ sustain rent levels much better compared to other properties. Younger buildings experience rent increases, compared to substantial rent decreases

Figure A4: Net Effective Rent on New Leases By Building Class

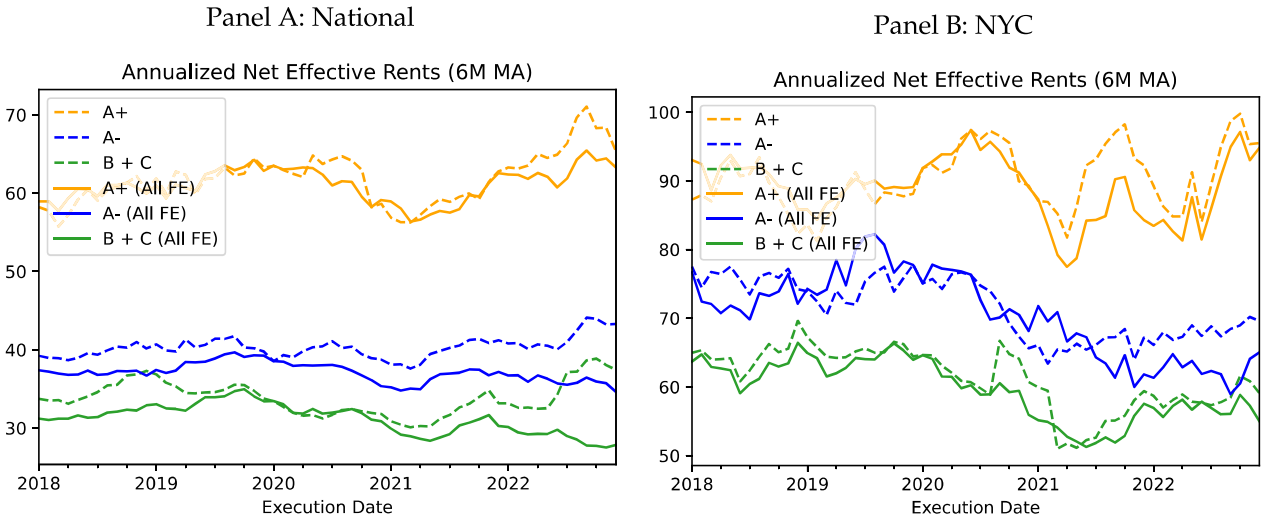

Notes: The figure shows annualized net effective rents on newly-signed leases for all markets (Panel A) and NYC (Panel B). Rents are shown rents by building class: A+ (in orange), A- (in blue), B+C (in green). Dashed lines denote raw data while solid lines remove tenant industry, renewal, and state plus major/non-major market fixed effects (Panel A) and tenant industry, renewal, and submarket fixed effects (Panel B). Data are sourced from CompStak.

for other properties. This divergence suggests a "flight to quality" in office demand in these markets.

Figure A5: Flight to Quality Defined by Building Age

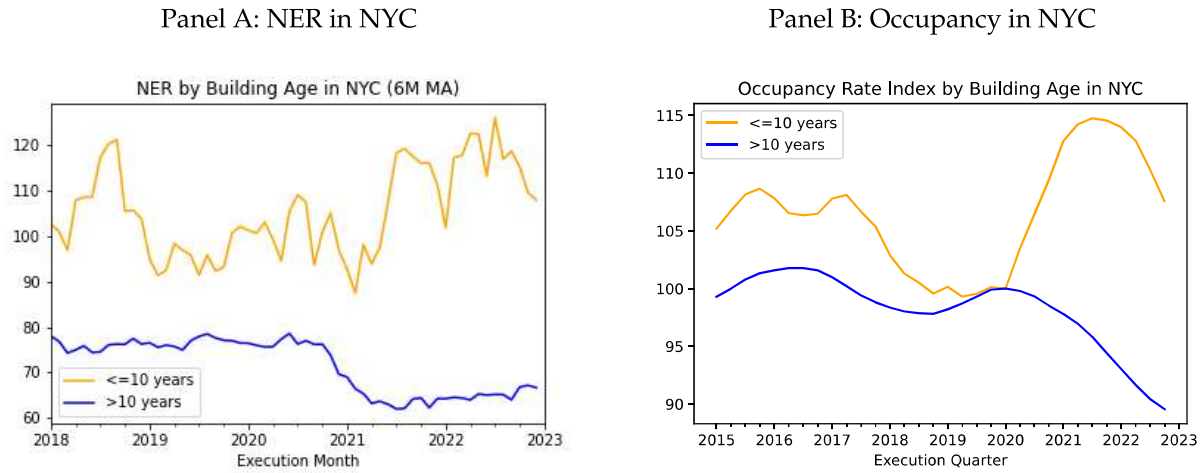

Notes: Panel A shows the annualized NER in December 2022 dollars in NYC. The graph shows the split by building age (age less than 10 years in orange, all others in blue). Panel B shows occupancy rates in NYC by building age. Data are sourced from CompStak.

Panel B of Figure A5 shows changes in occupancy, which is the other main driver of revenue. The graph breaks out trends in occupancy across buildings of different ages. Occupancy rates are scaled relative to their December 2019 levels. The clearest expression of quality differentiation reveals itself in the strong occupancy growth of the young buildings, while the older buildings struggle to retain tenants.

Table A1 provides detailed regression results of the relationship between building age and NER.

We control for month and submarket fixed effects (Column 1), and additionally for tenant fixed effects (Column 2). The specification in column 2 identifies the quality gradient from tenants that sign multiple leases, enabling a precise estimation of the association between age and rents. Each year of aging reduces NERs by $0.077 per sf in that specification. A building that is ten years older has 2.19% lower rents relative to the average rent of $35.2 per sf.

Table A1: Building Quality and Rent

	(1)	(2)	(3)	(4)	(5)	(6)	(7)
Building Age (Yrs)	-0.108***	-0.077***	-0.083***		-0.090***	-0.099***	-0.206***
	(0.016)	(0.015)	(0.014)		(0.015)	(0.028)	(0.051)
Building Age × Post Pandemic			-0.059***		-0.016	-0.093***	-0.118***
			(0.013)		(0.010)	(0.016)	(0.023)
Log Building Age				-0.083***			
				(0.006)			
Log Building Age × Post Pandemic				-0.036***			
				(0.007)			
Age × Post × Major Market					-0.056***		
					(0.013)		
Month FE	Yes	Yes	Yes	Yes	Yes	Yes	Yes
Submarket FE	Yes	Yes	Yes	Yes	Yes	Yes	Yes
Tenant FE	No	Yes	No	No	No	No	No
Sample	Full	Full	Full	Full	Full	Major Market	SF+NYC
N	126,024	53,409	126,024	125,884	126,024	45,852	9,751

Notes: This table estimates the relationship between property quality, measured by age, and net effective rent (NER). The dependent variable is NER expressed in 2022 dollars, except in column (4) in which the dependent variable is log(NER). The right-hand side controls always include the month of lease commencement and submarket fixed effects. The additional control is a fixed effect for tenant identity (not available for all leases). The sample includes leases signed from 2018–2022 for all columns. Column (6) additionally subsets to major markets, which include NYC, Philadelphia, Boston, Houston, Dallas, Austin, Nashville, Chicago, Atlanta, Miami, Washington D.C., Denver, Los Angeles, and San Francisco. Column (7) additionally subsets to NYC and San Francisco. To illustrate the changing premium on quality, we introduce an interaction with an indicator variable *Post* which is one after March 2020. Standard errors, in parentheses, are double clustered at the month of lease commencement and submarket level. * $p < 0.10$, ** $p < 0.05$, *** $p < 0.01$

Our key test is how this relationship changes after March 2020, represented as an interaction term with *Post* in column 3. This specification compares rent outcomes for leases signed in March 2020 and later, relative to leases signed between January 2018 and February 2020. We observe that interaction of building age and a post-pandemic indicator variable is negative and significant, indicating that young buildings become even more valuable after the pandemic. The quality premium increases. Column 4 uses log NER and log building age, and shows an additional 3.6% point rent elasticity to age, a 43% increase over the elasticity in the earlier period. Columns 5 and 6 show that this association is largely driven by shifts in major markets, and Column 7 shows that it is particularly large in NYC and San Francisco.

A3 Relationship between office demand and remote job postings

As an alternative measure of firms' remote working plans, we use job posting data from Ladders. This data allows us to measure the fraction of a firm's job listings that are for fully-remote positions. The Ladders data contains a flag indicating whether the position is remote or not. We then estimate the relationship between the change in office demand, measured as the percentage change in active lease space in square feet normalized by employment growth since January 2020, and the fraction of job postings that are remote. We merge job postings and tenant data for 135 large tenants.

Table A2 reports the results. The change in office demand is measured over various periods ranging from the last 3 to the last 24 months (relative to the time of data collection in February 2022). We find a significant negative relationship at all horizons. Our results suggest that firms that express a greater remote work preference in job listings have lower demand for office space. A 10% point increase in the share of remote job postings lowers office demand by 3.9–4.9% points. This result is consistent with the idea that durable shifts in remote work are changing the demand for office space.

Table A2: Remote Listings and Office Demand

	(1)	(2)	(3)
	Δ Space	Δ Space	Δ Space
Remote Listings (3 months)	-0.392**		
	(-2.41)		
Remote Listings (12 months)		-0.492**	
		(-2.46)	
Remote Listings (24 months)			-0.468**
			(-2.01)
Constant	-0.0123	-0.0106	-0.0156
	(-0.61)	(-0.52)	(-0.77)
Observations	135	135	135
R^2	0.042	0.044	0.030

t statistics in parentheses.

* $p < 0.10$, ** $p < 0.05$, *** $p < 0.01$

Notes: The dependent variable, Δ Space, is constructed from CompStak and defined as the square feet (sf) of leases executed post-pandemic minus the positive part of the difference between sf of leases expired post-pandemic and sf of leases commenced post-pandemic, and normalized by pre-pandemic active sf. The independent variables measure the ratio of remote job postings for a specific tenant within a time window since we downloaded the data snapshot from Ladders in February 2022. More specifically, we look at December 2021 to February 2022, January 2021 to February 2022 and January 2020 to Feb 2022 and check the ratio of tenants' remote jobs over their total job postings.

A4 Relationship between Bank Size and CRE Exposure

In this section, we examine the relationship between bank size and banks' commercial real estate (CRE) exposure using Call Report data. As part of mandatory quarterly reporting, U.S. commercial banks' Call Reports contain bank size, measured as bank book assets, and their outstanding commercial real estate loans for each quarter end. We measure CRE loans using the variable "UBPRD489". UBPRD489 contains the sum of construction and land development loans, nonfarm nonresidential mortgages, unsecured loans to finance commercial real estate, construction and land development, other real estate owned, and investments in unconsolidated subsidiaries and associated companies.

Table A3 reports various categories of bank size (Column 1), the number of banks in each group (Column 2), the fraction of aggregate bank assets the group represents (Column 3), the asset-weighted average (awa) ratio of CRE loans to bank assets (Column 4), and the fraction of aggregate CRE loans held by banks in that group (Column 5).

We find that medium and small banks are most exposed to CRE risks, with average exposures of around 20-25%, while the largest banks with over $250 billion assets have only moderate CRE exposure ($< 5\%$). Nonetheless, the dollar value of their CRE exposure still accounts for 24.3% of all CRE loans.

Table A3: Commercial Real Estate Exposure by Bank Size

(1) Bank Size ($ bi)	(2) Count	(3) Asset Share (%)	(4) CRE/Asset (%, awa)	(5) Exposure Share (%)
>250	13	55.5	4.5	24.3
100–250	22	15.2	7.9	11.5
50–100	16	4.9	17.7	8.4
25–50	34	5.0	18.7	9.0
10–25	73	5.0	24.4	11.7
2–10	399	7.0	25.5	17.2
0.5–2	1,198	4.8	28.0	13.1
<0.5	3,041	2.6	19.5	4.9

B Calibrating the Market Price of WFH Risk

We begin by creating a WFH factor which goes long stocks that benefit from the adoption of WFH and shorts stocks that suffer from that transition (Section B1). We then model the risk in office stock returns (REITs), estimating their exposure to the WFH factor (Section B2). We estimate the market price of WFH risk from the cross-section of office REITs (Section B3). Finally, Section B4 explains how we calibrate the SDF component M^{WFH} so that the model correctly prices the WFH risk factor.

B1 Constructing a WFH Equity Risk Factor

We form a portfolio that goes long stocks which benefit from remote work and short stocks which suffer from the move to WFH. This entails long positions in the technology and health care sectors, and short positions in the transportation, entertainment, and hotel sectors. The WFH factor composition can be found in Table B1. Several variations on the WFH factor construction, such as excluding entertainment stocks or just going long technology stocks and short transportation stocks, give similar results.

The WFH factor is a monthly rebalanced, long-short market capitalization weighted basket of stocks. On the last working day r of each month, which we call the rebalance day, each stock i in the long leg is assigned a weight $w_{i,l,r}$ and each stock j in the short leg is assigned a weight $w_{j,s,r}$

$$w_{i,l,r} = \frac{S_{i,r-1}}{\sum_{k \in c_{l,r}} S_{k,r-1}}; \quad w_{j,s,t} = \frac{S_{j,r-1}}{\sum_{k \in c_{s,r}} S_{k,r-1}}$$

Where $S_{k,r-1}$ is the market capitalization of stock k on day $r-1$, the working day immediately preceding rebalance day r, and $c_{l,r}$ and $c_{s,r}$ are the constituents in long and short legs respectively for rebalance date r. Further, we impose weight caps of 10% on each stock in the long leg and 20% on each stock in the short leg. The remaining weights are redistributed among remaining stocks of that leg in the same proportion above, i.e. proportional to their market capitalization, such that:

$$\sum_{k \in c_{l,r}} w_{k,l,r} = 1; \sum_{k \in c_{s,r}} w_{k,s,r} = 1$$

Once weights are assigned, daily returns of the long and short leg are calculated as follows:

$$R_{l,t} = \sum_{k \in c_{l,r_t}} w_{k,l,r_t} \left(\frac{P_{k,t}}{P_{k,t-1}} - 1 \right), \quad R_{s,t} = \sum_{k \in c_{s,r_t}} w_{k,s,r_t} \left(\frac{P_{k,t}}{P_{k,t-1}} - 1 \right)$$

Where $R_{l,t}$ and $R_{s,t}$ are the returns of the long and short legs of the Index and $P_{k,t}$ is the price of stock i on day t. w_{k,x,r_t} is the weight of stock k in leg x on date t, if t is a rebalance date and the weight of stock k in leg x on the rebalance date immediately preceding date t otherwise.

The daily return Ret_t^{wfh} on the WFH Index on date t is then given by $Ret_t^{wfh} = R_{l,t} - R_{s,t}$, whereas the level of the WFH index on date t, WFH_t, is given by:

$$WFH_t = WFH_{t-1}(1 + Ret_t^{wfh}); WFH_0 = 100$$

We start the WFH factor time series on December 31, 2014 since the composition of the WFH index is relatively stable after that date. Prior to 2015, many of the companies in the long or short leg were not trading, such as Zoom. Several perturbations on the WFH index construction deliver similar results. Figure B1 plots the WFH index constructed from weekly and monthly returns, starting from 100 on 12/31/20014.

Figure B1: Working From Home Risk Factor

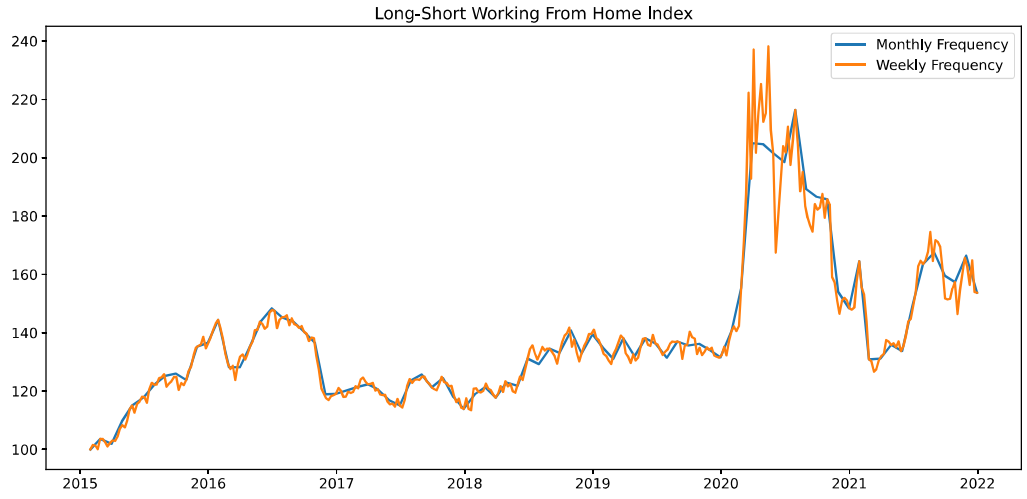

Before 2020, the WFH factor has modestly positive returns. It then spikes up 50% in early 2020 when large parts of the economy transition to remote work. Companies supporting remote work practices (Zoom, Peloton, etc.) flourish, while companies that require travel of physical proximity sell off (cruise lines, hotels, etc.). The WFH factor spikes up again in late 2021 when there is a renewed reduction in physical office occupancy (recall Figure 2). Naturally, the average realized return of the WFH factor

during the post-2020 period is strongly positive.

B2 Estimating WFH Risk Exposure for Office Market

To help understand how expected returns (risk premia) on office properties were affected during the pandemic, we propose the following simple model for the expected log return on publicly-traded office companies r^o_t:

$$x_t \equiv \mathbb{E}_t[r^o_{t+1}] = r^f_t + \beta^m_t \lambda^m + \beta^b_t \lambda^b + \beta^{wfh}_t \lambda^{wfh} \tag{7}$$

Office companies, and the assets they own, are exposed to three sources of risk: aggregate stock market risk, aggregate bond market risk, and the systematic risk associated with WFH. In addition, their expected returns reflect the evolution of short-term nominal bond yields r^f_t. To capture the changes in the underlying risk structure during the pandemic, we allow the exposures of office REITS to vary over time.

To show that WFH risk emerged in full force during the pandemic, we estimate time-varying betas from 36-month rolling-window regressions for monthly office REIT index' excess returns:

$$r^o_{t+1} - r^f_t = \alpha_t + \beta^m_t (r^m_{t+1} - r^f_t) + \beta^b_t (r^b_{t+1} - r^f_t) + \beta^{wfh}_t r^{wfh}_{t+1} + e_{t+1} \tag{8}$$

where $r^{wfh}_{t+1} = \log\left(1 + Ret^{wfh}_{t+1}\right)$, and Ret^{wfh}_{t+1} was defined in Section B1.

Figure B2 shows the three estimated betas for the office REIT index in blue in the first three panels. It plots the R^2 of regression (8) in the bottom right panel. The patterns in the stock and bond betas of office REITS in the three-factor model (blue line) are similar to those in a two-factor model without the WFH factor (orange line) before 2020. However, after 2020, omission of the WFH factor leads one to overstate the stock market beta (top left panel) and understate the bond market beta (top right panel). The WFH beta in the bottom left panel is close to zero in February 2020, an exposure estimated over the 36-month window from March 2018 through February 2020. The β^{wfh} for Office REITS then starts a precipitous decline to around -0.5. It remains strongly negative, ending at -0.3 in December 2021. The bottom-right panel shows that the R^2 improves due to the inclusion of the WFH factor after 2020.

B3 Estimating the WFH Risk Price from Cross-Section of Office REITs

We estimate the market prices of risk on the WFH factor, λ^{wfh}, using the cross-section of 22 individual office REITs listed in Table B2.

Table B1: Composition of WFH Index

Panel A: Long Positions

Ticker	Name	Leg	Sector
ZM	Zoom Video Communications	Long	Communication
VZ	Verizon Communications Inc	Long	Communication
ATVI	Activision Blizzard Inc	Long	Communication
NTDOF	Nintendo Ltd	Long	Communication
EA	Electronic Arts Inc	Long	Communication
CSCO	Cisco Systems Inc	Long	Communication
MTCH	Match Group Inc	Long	Communication
EGHT	8X8 Inc	Long	Communication
VG	Vg Corp	Long	Communication
PANW	Palo Alto Networks Inc	Long	Communication
VMW	Vmware Inc	Long	Cloud Technologies
INSG	Inseeog Inc	Long	Cloud Technologies
ZS	Zscalar Inc	Long	Cloud Technologies
DBX	Dropbox	Long	Cloud Technologies
NTAP	Netapp Inc	Long	Cloud Technologies
OKTA	Okta Corp	Long	Cybersecurity
FTNT	Fortinet Inc	Long	Cybersecurity
REGN	Regeneron Pharmaceuticals	Long	Healthcare/Biopharma
GILD	Gilead Sciences Inc	Long	Healthcare/Biopharma
SRNE	Sorrento Therapeutics Inc	Long	Healthcare/Biopharma
AMGN	Amgen Inc	Long	Healthcare/Biopharma
NFLX	Netflix Inc	Long	Information Technology
GOOGL	Alphabet Inc	Long	Information Technology
FB	Meta Platforms Inc	Long	Information Technology
AMZN	Amazon.Com Inc	Long	Information Technology
MSFT	Microsoft Corp	Long	Information Technology
CTXS	Citrix Systems Inc	Long	Information Technology
PRGS	Progress Software Corp	Long	Information Technology
TEAM	Atlassian Corporation Inc	Long	Information Technology
NTNX	Nutanix Inc	Long	Information Technology
DOCU	Docusign	Long	Online Document Mgmt
BOX	Box Inc	Long	Online Document Mgmt
UPLD	Upland Software Inc	Long	Online Document Mgmt
PFE	Pfizer Inc	Long	Vaccine Candidates
MRNA	Moderna Inc	Long	Vaccine Candidates
BNTX	Biontech Se	Long	Vaccine Candidates
JNJ	Johnson & Johnson	Long	Vaccine Candidates
AZN	Astrazeneca Plc	Long	Vaccine Candidates
NVAX	Novavax Inc	Long	Vaccine Candidates
PTON	Peloton Interactive Inc	Long	Virtual Healthcare
TDOC	Teladoc Health Inc	Long	Virtual Healthcare

Panel B: Short Positions

SIX	Six Flags Entertainment Corp	Short	Entertainment
EB	Eventbrite Inc	Short	Entertainment
LYV	Live Nation Entertainment In	Short	Entertainment
WYNN	Wynn Resorts Ltd	Short	Entertainment
LVS	Las Vegas Sands Corp	Short	Entertainment
CZR	Caesars Entertainment Inc	Short	Entertainment
HLT	Hilton Worldwide Holdings In	Short	Hotels
MAR	Marriott International	Short	Hotels
H	Hyatt Hotels Corp	Short	Hotels
IHG	Intercontinental Hotels	Short	Hotels
DAL	Delta Air Lines Inc	Short	Transportation
UAL	United Airlines Holdings Inc	Short	Transportation
AAL	American Airlines Group Inc	Short	Transportation
LUV	Southwest Airlines Co	Short	Transportation
CCL	Carnival Corp	Short	Transportation
NCLH	Norwegian Cruise Line Holdin	Short	Transportation
UNP	Union Pacific Corp	Short	Transportation

Table B2: List of Office REITS

Office REIT	Ticker
Alexandria Real Estate Equities, Inc.	ARE
Brandywine Realty Trust	BDN
Boston Properties, Inc.	BXP
CIM Commercial Trust Corp	CMCT
Cousins Properties	CUZ
Columbia Property Trust Inc.	CXP
Easterly Government Properties	DEA
Equity Commonwealth	EQC
Empire State Realty Trust	ESRT
Franklin Street Properties Corp.	FSP
Highwoods Properties, Inc.	HIW
Hudson Pacific Properties, Inc.	HPP
Kilroy Realty Corporation	KRC
Corporate Office Properties Trust	OFC
Office Properties Income Trust	OPI
Piedmont Office Realty Trust, Inc.	PDM
Paramount Group, Inc.	PGRE
SL Green Realty Corp	SLG
Vornado Realty Trust	VNO
Douglas Emmett, Inc.	DEI
City Office REIT, Inc.	CIO
New York City REIT, Inc.	NYC

Figure B2: Risk Exposures of Office REITs During Covid with WFH

We use a two-stage Fama-MacBeth procedure. In the first stage using the time-series, we estimate 36-month rolling-window regressions of each REIT's return on the three factor returns; i.e., we estimate equation (8) for each REIT separately. In the second cross-sectional step, we regress the realized return each month on the betas for that month. The market price of risk estimates are the average of the monthly slope estimates of the second step. We use only the months prior to the onset of the pandemic (December 2014–December 2019) when computing this average. Since the WFH index saw unusually high realizations after 2019, inclusion of 2020-2021 return realizations would lead one to confuse realized returns with expected returns (while in fact the two are negatively correlated). We obtain $\hat{\lambda}^{wfh} = -7.0\%$ annualized (t-stat is -0.52 but the sample is too short to reliably estimate this coefficient). Repeating the exercise with weekly instead of monthly return data and the 52-week rolling window betas, we obtain $\hat{\lambda}^{wfh} = -10.2\%$ (t-stat is -0.84).

For the risk prices on stocks and bond, we use the sample average of the estimated risk premia in the post-1994 period: $\lambda^m = 7.81\%$ and $\lambda^b = 2.91\%$. For the WFH risk price we use $\lambda^{wfh} = -7.0\%$, as

estimated above from monthly data. We combine the three time-varying betas from Figure B2 with the market price of risk estimates to form the expected return on the office REIT index as per equation (7). Figure B3 plots the resulting expected return time series. While the contribution from stocks (orange) and bond market risk (yellow) shrinks over the course of 2020 because of the declining stock and bond betas, the contribution from the WFH risk exposure (purple) is substantial. WFH risk contributes about 2–3% points to the expected return on office during the pandemic.

Figure B3: Expected Return of Office REITs During Covid

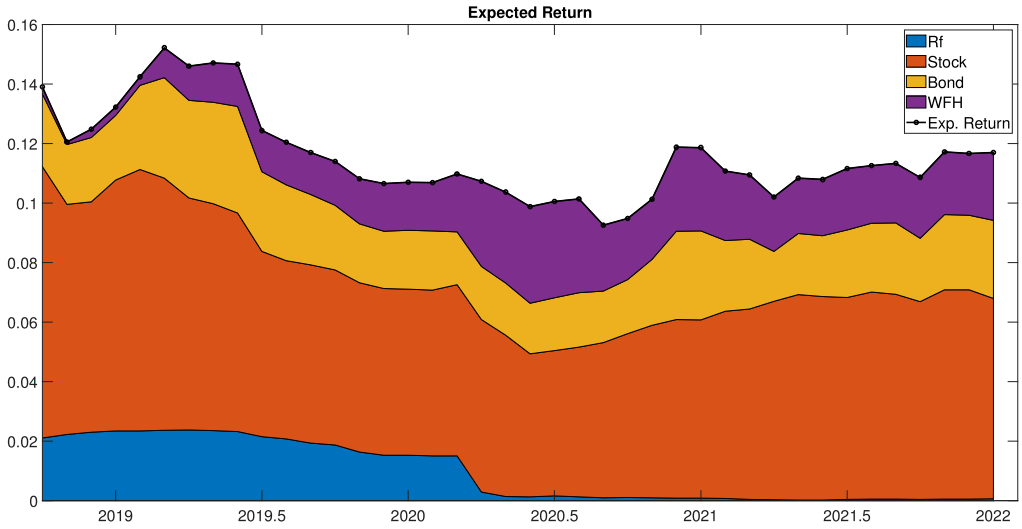

B4 Calibration M^{WFH}

In order to calibrate how WFH risk is priced, we match the data on the WFH risk factor. Specifically, we use data from the period December 2014–December 2019 to measure the conditional expected return on the WFH factor $Ret^{wfh}(z' = \text{low-WFH}|z = \text{low-WFH})$. We recognize that the WFH factor itself may be exposed to stock and bond market risk, as captured by the first two terms below, as well as to WFH risk, as captured by the last term:

$$Ret^{wfh}(z' = \text{low-WFH}|z = \text{low-WFH}) = \beta^m \lambda^m + \beta^b \lambda^b + \lambda^{wfh}.$$

We estimate the (conditional) stock and bond betas in the December 2014–December 2019 period. Appendix B3 showed how we pin down the (conditional) market prices of risk for the WFH, stock, and bond risk factors. Given our value of $\lambda^{wfh} = -7.0\%$, we find $Ret^{wfh}(z' = \text{low-WFH}|z = \text{low-WFH}) =$

-6.42%.

We use the data from December 2019 to December 2020 to measure the conditional expected return $Ret^{wfh}(z' = \text{high-WFH}|z = \text{low-WFH})$. This results in $Ret^{wfh}(z' = \text{high-WFH}|z = \text{low-WFH}) = 30.84\%$. Given that we only observe one such transition, we are forced to take this simpler approach.

Given that we have no data on the transition from the high-WFH to the low-WFH state and only two annual observations on the return conditional on remaining in the high-WFH state, we opt to assume that the second row of M^{WFH}, conditional on $z = \text{low-WFH}$, is equal to the first row, conditional on $z = \text{high-WFH}$.

We normalize the SDF entry $M^{WFH}(\text{low-WFH}|\text{low-WFH}) = 1$. This then leaves us with one equation in one unknown. We set $M^{WFH}(\text{high-WFH}|\text{low-WFH})$ to satisfy the Euler equation for the WFH equity risk factor for $z = \text{low-WFH}$:

$$1 = \left(\sum_{z'} \pi^{WFH}(z'|z) M^{WFH}(z'|z) Ret^{wfh}(z'|z) \right).$$

C Model Derivation

This section contains the full derivation of the model in Section 3. The goal is to solve the following equation:

$$\begin{aligned} V_t &= E_t\left[\sum_{j=1}^{\infty} M_{t,t+j}\left(Rev_{t+j} - Cost_{t+j}\right)\right] = E_t\left[\sum_{j=1}^{\infty} M_{t,t+j} Rev_{t+j}\right] - E_t\left[\sum_{j=1}^{\infty} M_{t,t+j} Cost_{t+j}\right] \\ &= V_t^R - V_t^C. \end{aligned}$$

First, we solve the revenue side, i.e., for V_t^R

C1 Revenue

Reproducing the equation for the law of motion for occupied space, Q_{t+1}^O below:

$$Q_{t+1}^O(Q_t^O, z') = min\{Q_t^O(1-\chi) + Q_t^O \chi s_{t+1}^O(z') + (\bar{Q}_t - Q_t^O)s_{t+1}^V(z'), \bar{Q}_{t+1}\}$$

From the stochastic process of the growth of the total space in the building we get:

$$\frac{\bar{Q}_{t+1}}{\bar{Q}_t} - 1 = \eta_{t+1}(z') \quad \Rightarrow \quad \bar{Q}_{t+1} = \bar{Q}_t(1 + \eta_{t+1}(z'))$$

and the scaled state variable $\hat{Q}_t^O$, we can be rearranged as

$$\hat{Q}_t^O = \frac{Q_t^O}{\bar{Q}_t} \quad \Rightarrow \quad Q_t^O = \hat{Q}_t^O \bar{Q}_t.$$

To convert $Q_{t+1}^O(Q_t^O, z')$ as a function of scaled variables, $Q_{t+1}^O(\hat{Q}_t, z')$, we substitute equations for $\bar{Q}_{t+1}$ and Q_t^O,

$$\hat{Q}_{t+1}^O \bar{Q}_t(1 + \eta_{t+1}(z')) = min\{\hat{Q}_t^O \bar{Q}_t(1-\chi) + \hat{Q}_t^O \bar{Q}_t \chi s_{t+1}^O(z') + (\bar{Q}_t - \hat{Q}_t^O \bar{Q}_t)s_{t+1}^V(z'), \bar{Q}_t(1 + \eta_{t+1}(z'))\}$$

$$\hat{Q}_{t+1}^O = min\{\frac{\hat{Q}_t^O(1-\chi) + \hat{Q}_t^O \chi s_{t+1}^O(z') + (1 - \hat{Q}_t^O)s_{t+1}^V(z'))}{1 + \eta_{t+1}(z')}, 1\}$$

Next, the rent revenue in the building/market in period $t+1$ is,

$$Rev_{t+1}(Q_t^O, R_t^O, z') = Q_t^O(1-\chi)R_t^O + \left[Q_t^O \chi s_{t+1}^O(z') + (\bar{Q}_t - Q_t^O)s_{t+1}^V(z')\right] R_{t+1}^m.$$

To derive the law of motion for R_t^O, we rewrite Rev_{t+1} as,

$$Q_{t+1}^O R_{t+1}^O = Q_t^O(1-\chi)R_t^O + \Big[Q_t^O \chi s_{t+1}^O(z')R_{t+1}^m + (\overline{Q}_t - Q_t^O)s_{t+1}^V(z')R_{t+1}^m\Big]$$

Dividing by Q_{t+1}^O we get,

$$R_{t+1}^O = \frac{Q_t^O}{Q_{t+1}^O}(1-\chi)R_t^O + \Big[\frac{Q_t^O}{Q_{t+1}^O}\chi s_{t+1}^O(z')R_{t+1}^m + \Big(\frac{\overline{Q}_t}{Q_t^O} - 1\Big)\frac{Q_t^O}{Q_{t+1}^O}s_{t+1}^V(z')R_{t+1}^m\Big]$$

which is the law of motion of R_t^O.

The growth rate of the market's NER per sqft is a stochastic process, which follows the following law of motion,

$$\frac{R_{t+1}^m}{R_t^m} - 1 = \epsilon_{t+1}(z') \quad \Rightarrow \quad R_{t+1}^m = R_t^m(1+\epsilon_{t+1}(z')).$$

We define the state variable $\hat{R}_t^O$ as,

$$\hat{R}_t^O = \frac{R_t^O}{R_t^m}.$$

Next, we want to find the law of motion for the scaled state variable $\hat{R}_{t+1}^O$:

$$\widehat{R}_{t+1}^O = \frac{Q_t^O}{Q_{t+1}^O}(1-\chi)\frac{R_t^O}{R_{t+1}^m}\frac{R_t^m}{R_t^m}\frac{\overline{Q}_{t+1}}{\overline{Q}_{t+1}}\frac{\overline{Q}_t}{\overline{Q}_t} + \Big[\chi s_{t+1}^O(z')\frac{Q_t^O}{\overline{Q}_t}\frac{\overline{Q}_t}{\overline{Q}_{t+1}}\frac{\overline{Q}_{t+1}}{Q_{t+1}^O} + s_{t+1}^V(z')\frac{Q_t^O}{\overline{Q}_t}\frac{\overline{Q}_t}{\overline{Q}_{t+1}}\frac{\overline{Q}_{t+1}}{Q_{t+1}^O}\Big(\frac{1-\widehat{Q}_t^O}{\widehat{Q}_t^O}\Big)\Big]$$

$$\widehat{R}_{t+1}^O(\widehat{R}_t^O, \widehat{Q}_t^O, \widehat{Q}_{t+1}^O, z') = \frac{(1-\chi)\widehat{R}_t^O}{(1+\epsilon_{t+1}(z'))(1+\eta_{t+1}(z'))}\frac{\widehat{Q}_t^O}{\widehat{Q}_{t+1}^O} + \Big[\frac{\chi s_{t+1}^O(z')}{(1+\eta_{t+1}(z'))}\frac{\widehat{Q}_t^O}{\widehat{Q}_{t+1}^O} + \frac{s_{t+1}^V(z')(1-\widehat{Q}_t^O)}{(1+\eta_{t+1}(z'))\widehat{Q}_{t+1}^O}\Big]$$

We define scaled revenues as

$$\widehat{Rev}_{t+1}(\hat{Q}_t^O, \hat{R}_t^O, z') = \frac{Rev_{t+1}}{\bar{Q}_t R_t^m}.$$

Rewriting the equation for $Rev_{t+1}(Q_t^O, R_t^O, z')$:

$$Rev_{t+1}(\hat{Q}_t^O, \hat{R}_t^O, z') = \hat{Q}_t^O\bar{Q}_t(1-\chi)\hat{R}_t^O R_t^m + \Big[\hat{Q}_t^O\bar{Q}_t\chi s_{t+1}^O(z') + (\bar{Q}_t - \hat{Q}_t^O\bar{Q}_t)s_{t+1}^V(z')\Big]R_t^m(1+\epsilon_{t+1}(z'))$$

$$Rev_{t+1}(\hat{Q}_t^O, \hat{R}_t^O, z') = \bar{Q}_t R_t^m\Big[\hat{Q}_t^O(1-\chi)\hat{R}_t^O + \Big[\hat{Q}_t^O\chi s_{t+1}^O(z') + (1-\hat{Q}_t^O)s_{t+1}^V(z')\Big](1+\epsilon_{t+1}(z'))\Big].$$

Scaled Revenue $\widehat{Rev}_{t+1}$ can be written as

$$\widehat{Rev}_{t+1}(\hat{Q}_t^O, \hat{R}_t^O, z') = \hat{Q}_t^O(1-\chi)\hat{R}_t^O + \left[\hat{Q}_t^O \chi s_{t+1}^O(z') + (1-\hat{Q}_t^O)s_{t+1}^V(z')\right](1+\epsilon_{t+1}(z')).$$

The expected present discounted value (PDV) of revenues is written as

$$V_t^R = E_t\Big[\sum_{j=1}^{\infty} M_{t,t+j} Rev_{t+j}\Big].$$

The scaled version of revenues can be written as:

$$\hat{V}_t^R = \frac{V_t^R}{\overline{Q}_t R_t^m},$$

which solves the following Bellman equation:

$$\hat{V}_t^R(\hat{Q}_t^O, \hat{R}_t^O, z) = \sum_{z'} \pi(z'|z) M(z'|z) \left[\widehat{Rev}_{t+1}(\hat{Q}_t^O, \hat{R}_t^O, z') + (1+\eta(z'))(1+\epsilon(z'))\hat{V}_{t+1}^R(\hat{Q}_{t+1}^O, \hat{R}_{t+1}^O, z')\right].$$

Finally, we get V_t^R by

$$V_t^R = \hat{V}_t^R(\hat{Q}_t^O, \hat{R}_t^O, z)\overline{Q}_t R_t^m.$$

C2 Costs

The building costs are written as:

$$Cost_{t+1} = C_{t+1}^{var}(z')Q_{t+1}^O + C_{t+1}^{fix}(z')\overline{Q}_{t+1} + \left[Q_t^O \chi s_{t+1}^O(z') LC_{t+1}^R(z') + (\overline{Q}_t - Q_t^O)s_{t+1}^V(z') LC_{t+1}^N(z')\right] R_{t+1}^m.$$

Substituting for R_{t+1}^m, we get,

$$\begin{aligned} Cost_{t+1} = {} & C_{t+1}^{var}(z')Q_{t+1}^O + C_{t+1}^{fix}(z')\overline{Q}_{t+1} + \\ & \left[\hat{Q}_t^O \bar{Q}_t \chi s_{t+1}^O(z') LC_{t+1}^R(z') + (\bar{Q}_t - \hat{Q}_t^O \bar{Q}_t)s_{t+1}^V(z') LC_{t+1}^N(z')\right] R_t^m(1+\epsilon_{t+1}(z')). \end{aligned}$$

We define scaled costs as:

$$\widehat{Cost}_{t+1} = \frac{Cost_{t+1}}{\bar{Q}_t R_t^m}.$$

Therefore, we have:

$$\widehat{Cost}_{t+1} = \frac{Cost_{t+1}}{\overline{Q}_t R_t^m}$$
$$= c_{t+1}^{var}(z')\widehat{Rev}_{t+1} + \left[c_{t+1}^{fix}(z')\widehat{R}_{t+1}^O(1+\eta(z')) + \hat{Q}_t^O \chi s_{t+1}^O(z') LC_{t+1}^R(z') + (1-\hat{Q}_t^O)s_{t+1}^V(z')LC_{t+1}^N(z')\right](1+\epsilon(z'))$$

where

$$c_{t+1}^{fix}(z') = \frac{C_{t+1}^{fix}(z')}{R_{t+1}^O} \qquad\qquad c_{t+1}^{var}(z') = \frac{C_{t+1}^{var}(z')}{R_{t+1}^O}.$$

The expected PDV of costs is written as:

$$V_t^C = E_t\Big[\sum_{j=1}^{\infty} M_{t,t+j} Cost_{t+j}\Big].$$

The scaled version is:

$$\hat{V}_t^C = \frac{V_t^C}{\overline{Q}_t R_t^m},$$

which solves the Bellman equation

$$\hat{V}_t^C(\hat{Q}_t^O, \hat{R}_t^O, z) = \sum_{z'} \pi(z'|z) M(z'|z) \left\{\widehat{Cost}_{t+1}(\hat{Q}_t^O, \hat{R}_t^O, z') + (1+\eta(z')(1+\epsilon(z'))\hat{V}_{t+1}^C(\hat{Q}_{t+1}^O, \hat{R}_{t+1}^O, z')\right\}.$$

Finally, we get V_t^C by

$$V_t^C = \hat{V}_t^C(\hat{Q}_t^O, \hat{R}_t^O, z)\overline{Q}_t R_t^m.$$

D Calibration Algorithm

The following describes the steps in the calibration algorithm for the universe of NYC office buildings (All NYC) and the subset of A+ buildings (NYC A+). We set the depreciation to 2.56% in both calibrations, equal to the depreciation rate of commercial properties for tax purposes of 39 years. The calibration for All NYC takes the persistence parameter of the WFH state, p, as given. This parameter is pinned down from the A+ calibration. Conversely, the calibration for NYC A+ takes the parameter $\Delta\eta$ as given. This parameter is pinned down from the All NYC calibration. Hence, the two calibrations are interdependent: they solve a fixed-point problem.

D1 All NYC, given p

1. Keep only office buildings and exclude subleases in the CompStak data set of leases for NYC.
2. Calculate the average lease term for all leases in NYC. Set χ equal to the reciprocal.
3. Estimate ε from data:
   (a) To estimate $\varepsilon(E)$ and $\varepsilon(R)$, first calculate NER series for each month controlling for submarket, tenant industry, leasing type, and building class FEs, and take the 6-month moving average. Use data from January 2000 (start of CompStak) until December 2019.
   (b) If more than 6 months of the 1-year rolling window falls in recession, then that rolling year is considered to be a recession; otherwise it is considered to be an expansion. We use the leasing cycle definition instead of the business cycle.
   (c) Compute the annual growth rate of the six-month moving average rent, and take the average separately for expansions and recessions.
   (d) Estimate $\epsilon(WFHR)$ as the annualized realized NER growth between March 2020 and December 2020, and $\epsilon(WFHE)$ as the annualized realized rent growth between December 2020 and December 2022.
4. Estimate $\eta(E)$ and $\eta(R)$ from data:
   (a) Compute the growth rate in floor space in year t as the newly constructed office square feet in year t relative to the total square feet of office space built before year t. We look at growth after 1950 for NYC All.

(b) Year t is a recession when more than six months of that year is in recession.

(c) We take the average the construction growth rate separately for expansions and recessions.

(d) Finally, we subtract the rate of depreciation to arrive at $\eta(E)$ and $\eta(R)$

5. Set $\eta(WFHE) = \eta(E) + \Delta\eta$ and $\eta(WFHR) = \eta(R) + \Delta\eta$. Find the $\Delta\eta$ such that the long-run growth rate of potential rent in the All NYC is zero:

$$\sum_z \pi(z)(1+\varepsilon(z))(1+\eta(z)) = 1,$$

where $\pi(z)$ is the 4×1 ergodic distribution of the 4×4 Markov Chain $\pi(z'|z)$.

6. Estimate the four parameters $\{s^O(E), s^O(R), s^V(E), s^V(R)\}$ to match the following four moments in quarterly Manhattan office occupancy rate data for from 1987.Q1 to 2019.Q4:

(a) empirical mean

(b) empirical standard deviation

(c) empirical min - 0.5%

(d) empirical max + 0.5%

7. Assume that the four parameters $\{s^O(WFHE), s^O(WFHR), s^V(WFHE), s^V(WFHR)\}$ are shifted by a common factor δ relative to their no-WFH counterparts: $s^{\{V,O\}}(WFH) = \delta \cdot s^{\{V,O\}}(no-WFH)$. Estimate the parameter δ to best fit the dynamics of the office occupancy rate in the 15 quarters from 2020.Q1–2023.Q3. The first 4 quarters are WFH-R and the last 11 are WFH-E. The dynamics are given by the model:

$$\hat{Q}^O_{t+1}(\hat{Q}^O_t, z') = \frac{s^V_{t+1}(z')}{1+\eta_{t+1}(z')} + \hat{Q}^O_t \cdot \frac{1-\chi+\chi s^O_{t+1}(z') - s^V_{t+1}(z')}{1+\eta_{t+1}(z')}$$

D2 NYC A+, given $\Delta\eta$

The calibration for the A+ office cash flows is based on the subset of leases in A+ buildings. It follows the same steps as outlined above for All NYC, with the following modifications:

4. When calculating η for A+ buildings, we collect all the buildings that have ever entered into the A+ universe, given our time-varying definition of A+ buildings, and re-do the calculation for NYC

All. Since A+ is only a subset of NYC market, we start the calculation of *eta* for each year from 1970 to 2019 to avoid extreme value caused by lack in coverage.

5. The NYC A+ calibration takes $\Delta\eta$ from the All NYC calibration.

6. We use data from NAREIT on the U.S. office sector occupancy from 2000.Q1 to 2019.Q4 to calibrate $\{s^O(E), s^O(R), s^V(E), s^V(R)\}$. We target a minimum occupancy rate that's lower than the empirical min in this sample period, because the A+ occupancy data is missing in the 1990s, which is the worst historical period for office occupancy. We assume that both A+ and the entire Manhattan office market experienced the same number of standard deviation decline from their mean since 2000 when they reached their own minimum in the 1990s.

8. Given all other parameters, find p to match the observed realized return on NYC-centric office REITS between December 31, 2019 and December 31, 2020, after adjusting for leverage. See the discussion in Section 3.4.

Figure D1 shows the valuation ratio for office $\widehat{V}$ conditional on expansion, recession, WFH-expansion and WFH-recession for the All NYC calibration. The x-axis plots the grid for $\widehat{Q}^O$ and the y-axis shows the grid for $\widehat{R}^O$. Office valuation ratios are increasing in both occupancy $\widehat{Q}^O$ and rent $\widehat{R}^O$.

D3 Inferring the Equity Premium in the high-WFH state

We back out the the equity market risk premium in the WFH-E and WFH-R states from the SDF calculated in Section 3.3.2. We assume that the 4×4 equity market return matrix equals the Kronecker product of two 2×2 equity return matrices. The first matrix, $Ret^{m,BC}(z'|z)$, governs the stock market return between expansions and recessions, and the second matrix, $Ret^{m,WFH}(z'|z)$, determines how that first return matrix shifts between the low-WFH and high-WFH states. We have already pinned down $Ret^{m,BC}(z'|z)$ by matching the historical equity risk premium in expansions and recessions. The resulting system of four Euler equations (one for each state z) is:

$$1 = \left(\sum_{z'} \pi(z'|z) M(z'|z) \left(Ret^{m,BC}(z'|z) \otimes Ret^{m,WFH}(z'|z) \right) \right)$$

We apply the following restriction:

Figure D1: $\hat{V}$ for All NYC Market by States

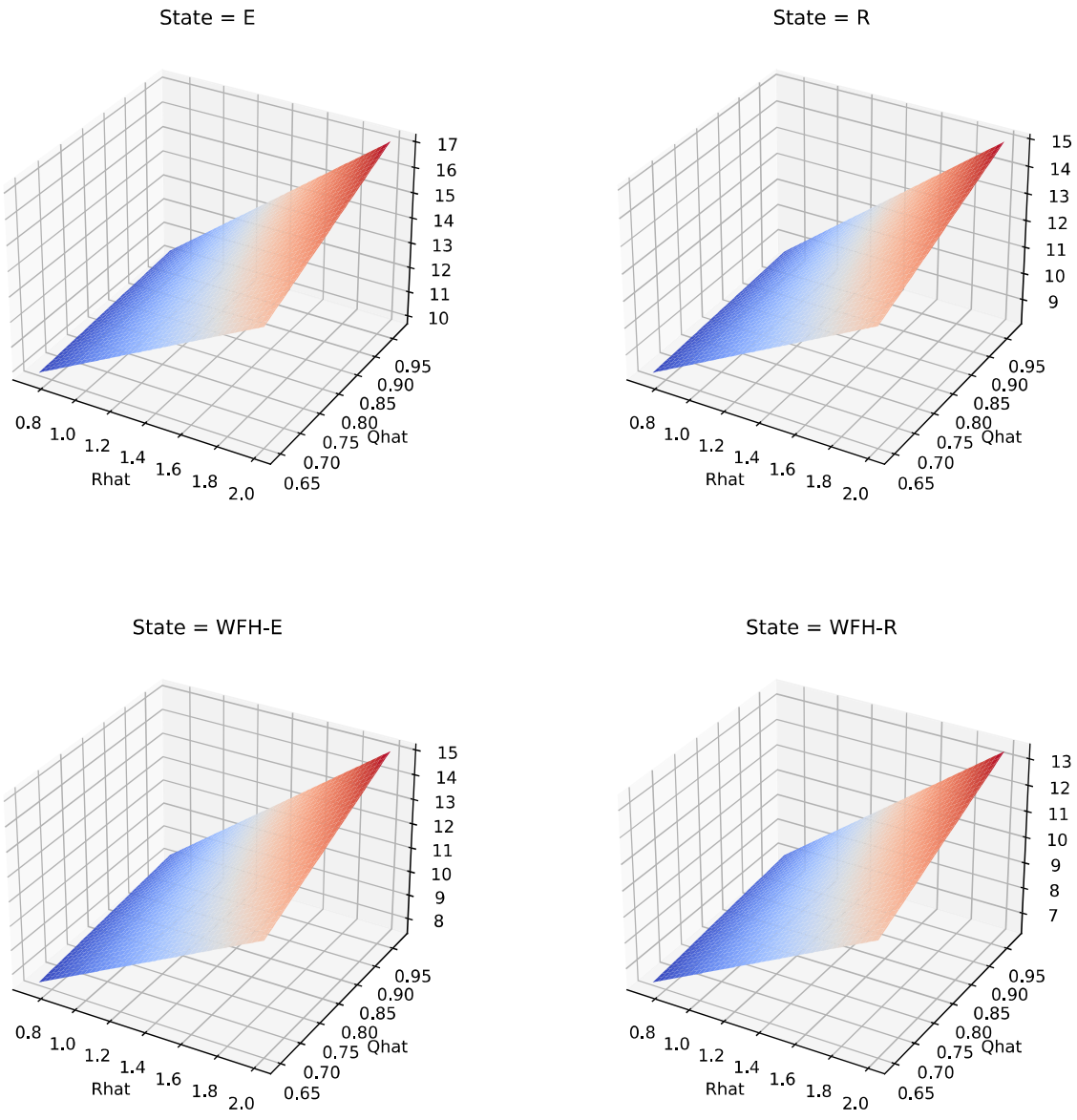

$$Ret^{m,WFH} = \begin{array}{c} \\ \text{low-WFH} \\ \text{high-WFH} \end{array} \begin{array}{c} \begin{array}{cc} \text{low-WFH} & \text{high-WFH} \end{array} \\ \begin{bmatrix} 1 & Ret^{m}_{NW} \\ Ret^{m}_{WN} & 1 \end{bmatrix} \end{array}.$$

We estimate the two unknowns Ret^{m}_{NW} and Ret^{m}_{WN} from two Euler equations (either the first and third or the second and fourth equations). Either pair generates very similar results.

E Results for NYC A+ Market

Table E1 shows the calibration of the cash-flow parameters for the A+ market segment, following the algorithm outlined in Appendix D. Naturally, the state transition and SDF matrices are the same for all properties.

Table E1: Calibration for NYC A+

Variable	Symbol	E	R	WFH-E	WFH-R
Market NER growth	ϵ	0.0598	-0.1389	0.0363	-0.0838
Supply growth	η	-0.0147	-0.0078	-0.0297	-0.0227
Lease renewal share	s^O	0.8586	0.6031	0.6459	0.4537
New leasing share	s^V	0.1075	0.1827	0.0809	0.1375

Table E2 shows the model solution for the A+ calibration. The model delivers a lower cap rate for A+ NYC office, due to the lower riskiness of A+ cash flows. Class A+ has lower vacancy levels than the NYC market as a whole, on average as well as in the WFH states.

Appendix Figure E1 shows the valuation ratio $\widehat{V}$ in each state as a function of occupancy and rent state variables.

Table E2: Model Solution for NYC A+ Calibration

Statistic	Uncond	E	R	WFHE	WFHR
Cap rate	0.0657	0.0629	0.0800	0.0630	0.0752
Office $\mathbb{E}[Ret] - 1$	0.0716	0.0606	0.1524	0.0469	0.1249
Office RP = $\mathbb{E}[Ret] - 1 - R_f$	0.0662	0.0617	0.1153	0.0480	0.0877
$\mathbb{E}[g_t]$	0.0008	0.0180	-0.0253	-0.0147	-0.0381
Vacancy rate $= 1 - \widehat{Q}^O$	0.1046	0.0818	0.1198	0.1330	0.1601
$\widehat{\text{Rev}}$	0.7966	0.8134	0.8245	0.7561	0.7659
$\widehat{\text{Cost}}$	0.3773	0.3835	0.3914	0.3602	0.3688
$\widehat{\text{NOI}} = \widehat{\text{Rev}} - \widehat{\text{Cost}}$	0.4192	0.4299	0.4331	0.3958	0.3971
$\widehat{V}^R$	12.3023	12.7131	11.8023	11.9482	11.0398
$\widehat{V}^C$	5.9246	6.0861	5.6780	5.8134	5.4006
$\widehat{V} = \widehat{V}^R - \widehat{V}^C$	6.3777	6.6270	6.1242	6.1348	5.6392

Figure E1: $\hat{V}$ for NYC A+ Market by States

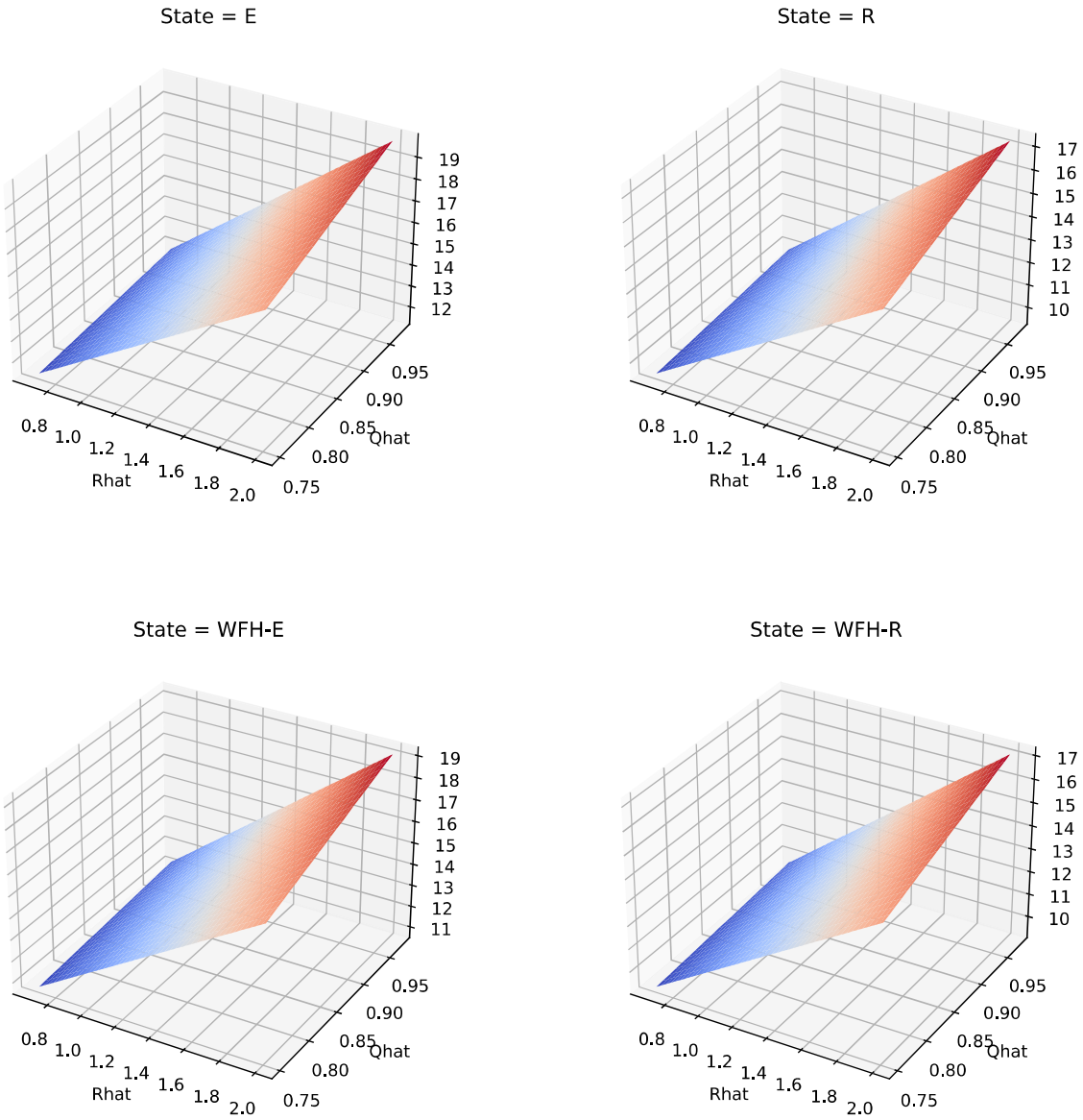

F Calibration to Other Markets

We repeat the calibration procedure discussed in the main text and in Appendix D for San Francisco and Charlotte. We use CompStak data to measure market rent growth, ε, before and during the pandemic. For Charlotte, we use data until May 2023 since its market moved up significantly since Dec 2022, which makes the WFHE calibration more representative of the average state of its market in WFHE. We also use CompStak data to measure pre-pandemic office construction rates (η is the construction minus the depreciation rate). Like in the NYC calibration, net supply growth rates during the pandemic (WFHR and WFHE) are set equal to their pre-pandemic counterparts (R and E) minus an adjustment factor (the same as NYC one). Due to the incomplete building coverage in CompStak, estimation of η for San Francisco and Charlotte starts in 1980. We use contractual occupancy rate data from Cushman and Wakefield to calibrate s^O and s^V before and during the pandemic [26]. We leave the office depreciation rate and the operational cost parameters the same as in the NYC calibration. Naturally, we assume that the dynamics of the aggregate state variable $\pi(z', z)$ are common across markets, as well as the market prices of risk $M(z', z)$.

Table F1 shows the calibrated parameters for San Francisco and F2 shows those for Charlotte. Table F3 and F4 show the main moments for San Francisco and Charlotte, respectively. The SF office market is riskier than the NYC market, featuring a rent cycle of greater amplitude which translates into a higher risk premium and cap rate. Charlotte is less risky than the SF market. Figure F1 plots fan charts for occupancy rates, revenues, NOI and cap rates for San Francisco and Charlotte.

Table F1: Calibration for San Francisco

Variable	Symbol	E	R	WFH-E	WFH-R
Market NER growth	ϵ	0.0953	-0.1782	-0.0287	-0.2189
Supply growth	η	-0.0183	-0.0104	-0.0332	-0.0253
Lease renewal share	s^O	0.8552	0.4834	0.3841	0.2171
New leasing share	s^V	0.2337	0.4374	0.1050	0.1965

[26] The CWK data of SF and Charlotte starts from 2008 and 2014. We impute their occupancy between 2005 and the sample start by regressing CWK occupancy on log NER and city FE in the top 20 city sample. We use 82% as the empirical min for SF based on the estimation from Krainer et al. (2001), and we use 80.6% for Charlotte based on https://www2.census.gov/library/publications/1997/compendia/statab/117ed/tables/construc.pdf.

Table F2: Calibration for Charlotte

Variable	Symbol	E	R	WFH-E	WFH-R
Market NER growth	ϵ	0.0417	-0.1790	0.0716	-0.1516
Supply growth	η	0.0023	0.0199	-0.0126	0.0050
Lease renewal share	s^O	0.9408	0.9408	0.6177	0.6177
New leasing share	s^V	0.2084	0.1283	0.1368	0.0842

Table F3: Model Solution for San Francisco Calibration

Statistic	Uncond	E	R	WFHE	WFHR
Cap rate	0.1042	0.0946	0.1250	0.1069	0.1398
Office $\mathbb{E}[Ret] - 1$	0.1066	0.0924	0.2074	0.0804	0.1574
Office RP = $\mathbb{E}[Ret] - 1 - R_f$	0.1012	0.0935	0.1703	0.0815	0.1202
$\mathbb{E}[g_t]$	-0.0130	0.0396	-0.0360	-0.0898	-0.1124
Vacancy rate $= 1 - \widehat{Q}^O$	0.1982	0.1059	0.1628	0.3682	0.3652
$\widehat{\text{Rev}}$	0.8057	0.8478	0.8255	0.7178	0.7693
$\widehat{\text{Cost}}$	0.4188	0.4214	0.4142	0.4115	0.4382
$\widehat{\text{NOI}} = \widehat{\text{Rev}} - \widehat{\text{Cost}}$	0.3868	0.4265	0.4113	0.3063	0.3311
$\widehat{V}^R$	7.8474	8.8025	7.8631	6.2366	6.1456
$\widehat{V}^C$	4.0956	4.4742	4.0028	3.4992	3.4294
$\widehat{V} = \widehat{V}^R - \widehat{V}^C$	3.7518	4.3282	3.8603	2.7374	2.7163

Table F4: Model Solution for Charlotte Calibration

Statistic	Uncond	E	R	WFHE	WFHR
Cap rate	0.0750	0.0744	0.0996	0.0631	0.0856
Office $\mathbb{E}[Ret] - 1$	0.0934	0.0711	0.1792	0.0790	0.1980
Office RP = $\mathbb{E}[Ret] - 1 - R_f$	0.0880	0.0723	0.1421	0.0802	0.1608
$\mathbb{E}[g_t]$	0.0100	0.0282	-0.0326	0.0056	-0.0559
Vacancy rate $= 1 - \widehat{Q}^O$	0.1559	0.1005	0.1338	0.2516	0.2866
$\widehat{\text{Rev}}$	0.8445	0.9083	0.9191	0.7076	0.7153
$\widehat{\text{Cost}}$	0.4203	0.4426	0.4469	0.3716	0.3785
$\widehat{\text{NOI}} = \widehat{\text{Rev}} - \widehat{\text{Cost}}$	0.4242	0.4657	0.4723	0.3360	0.3367
$\widehat{V}^R$	11.5274	12.2595	10.8674	10.7801	9.3437
$\widehat{V}^C$	5.9060	6.1478	5.4516	5.7902	5.0634
$\widehat{V} = \widehat{V}^R - \widehat{V}^C$	5.6214	6.1117	5.4157	4.9899	4.2803

Figure F1: Fan Charts for San Francisco and Charlotte

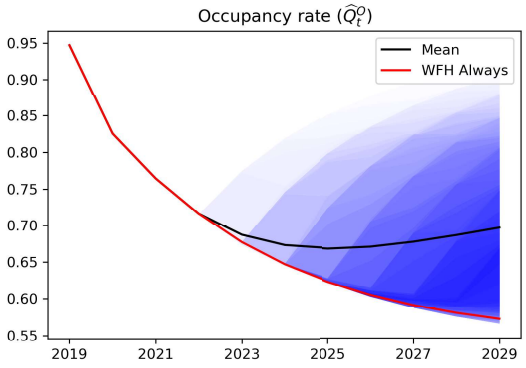

(a) San Francisco: Occupancy

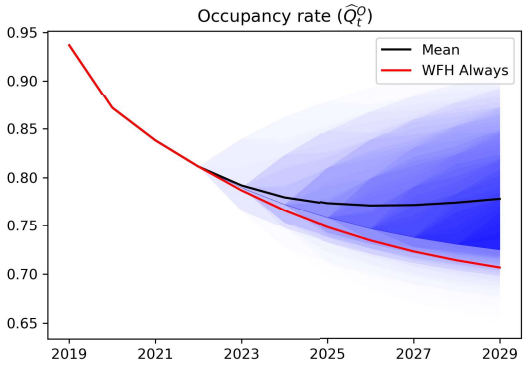

(b) Charlotte: Occupancy

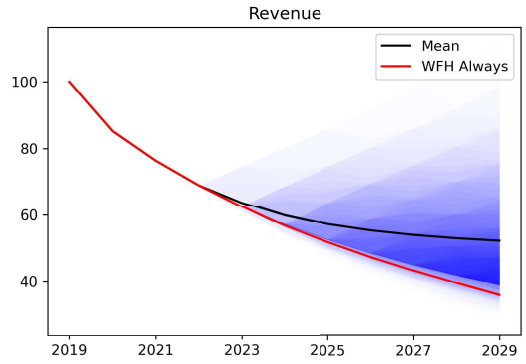

(c) San Francisco: Revenue

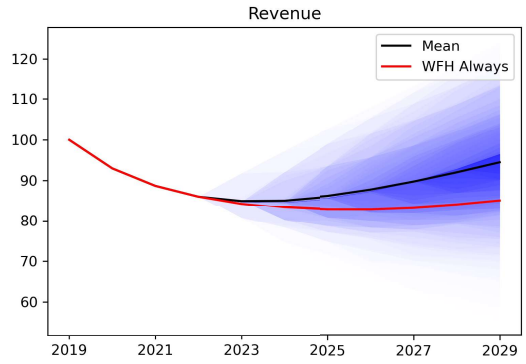

(d) Charlotte: Revenue

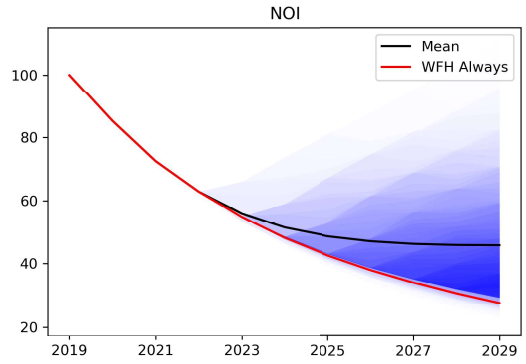

(e) San Francisco: NOI

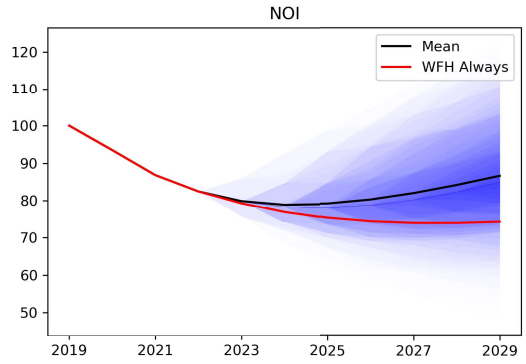

(f) Charlotte: NOI

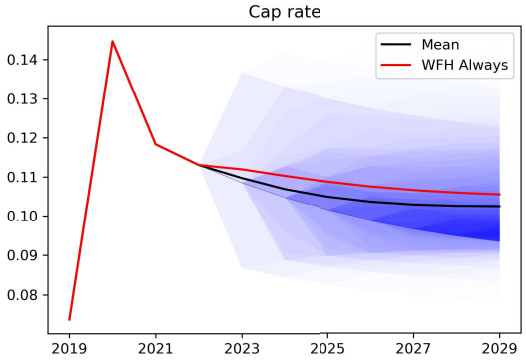

(g) San Francisco: Cap Rate

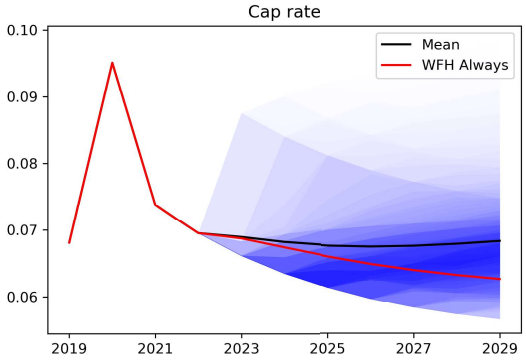

(h) Charlotte: Cap Rate

G Additional Model Results

G1 Term Structure of Valuations

We can decompose the (change in) office value into the contribution from each of the future cash flows. Figure G1 plots the share of the total value of office that comes from each of the first 20 years of cash flows. The lines are downward sloping as cash flows in the near term are more valuable than cash flows farther in the future due to discounting. Each line refers to a different current state for the economy. Interestingly, in expansions (such as 2019) the contribution of the nearest-term cash flows is much smaller than in the WFH-R state (such as 2020). For the share of short-term in total cash flows to rise (in present-value) between 2019 and 2020, the value of the cash flows in the farther future must fall by more than in the near future. This occurs because rents (and NOI) in the short-term are largely locked in given the long-term nature of leases. Investors would be willing to pay a premium for buildings that have a lot of long-term pre-pandemic leases in place.

This pattern is unusual, compared to the equity markets, where van Binsbergen, Brandt and Koijen (2012) find that the share of short-maturity equity cash flows falls in the mild recession of 2001, indicating an expected rebound in the near term, and stays flat in the deep recession of 2008, indicating a near-permanent shock to cash flows. Our results therefore suggest that the locked-in nature of commercial leases results in a different term structure of cash flow shocks in commercial real estate compared to other asset classes. In turn, this suggests that the shock to commercial office as a result of remote work may play out over an extended horizon.

Figure G1: Decomposing Office Values by Horizon

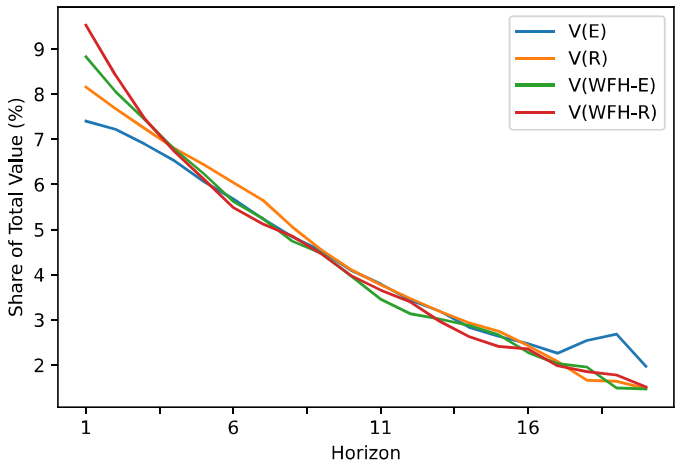

G2 Sensitivity to WFH-R Rent Growth

Figure G2 shows the office valuation for NYC under an alternative assumption on NER growth in the WFH-R state, namely that it equals the NER growth in a regular recession state R. The impact on the model prediction is modest.

Figure G2: Setting $\epsilon(WFH - R) = \epsilon(R)$

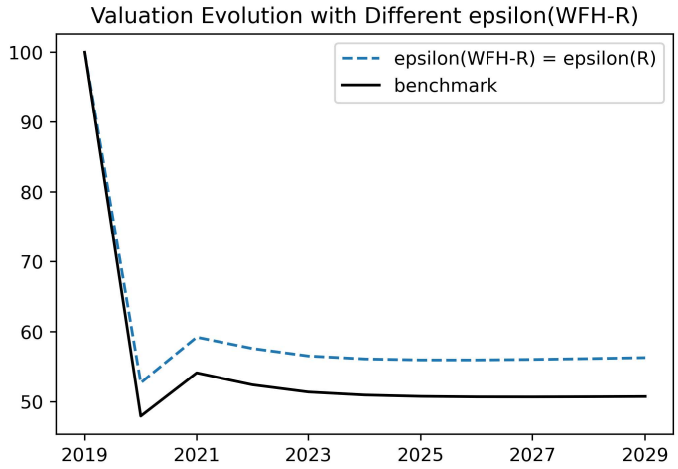

G3 Shutting Down WFH Risk Channel

Figure G3 shows the valuation impact in a model where there is no priced WFH risk. We compute this model by setting the component of the SDF that encodes WFH risk equal to the identity matrix: $M^{WFH} = 1$. The impact on the value decline of NYC office is -48.1% in 2020 and -44.8% in 2029, relative to pre-pandemic levels. The corresponding numbers in the benchmark model are -52.0% and -49.2%.

G4 Robustness Tests for San Francisco

Figure G4 performs four sensitivity analyses for San Francisco changing (i) rent growth in the WFH-E state $\varepsilon(WFH - E)$, a state in which the model spends a lot of time conditional on making the transition to a WFH state (panel a), (ii), the gap between net supply growth in the WFH relative to the no-WFH states $\Delta\eta$ (panel b), (iii), the persistence of remote work p, and (iv), introducing a floor for office values set at 30% of pre-pandemic valuations. The latter exercise is a simple way to model additional optionality from adaptive reuse not already captured by the net supply parameter η. This specification is intended to capture the redeployability option, as in Kim and Kung (2017) and Benmelech, Garmaise and Moskowitz

Figure G3: Shutting Down the Risk Channel

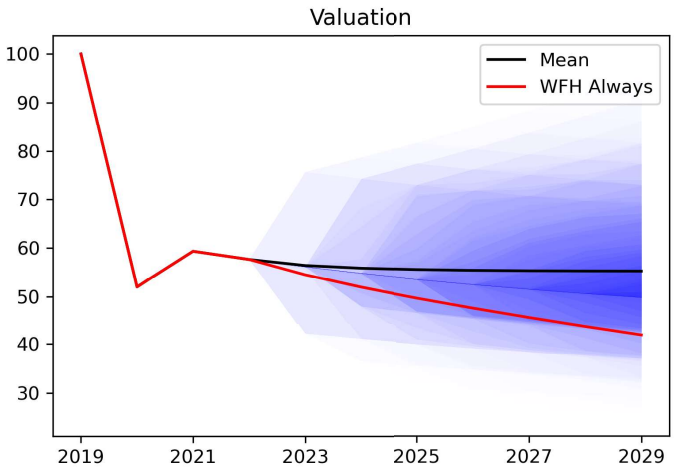

(2005), as office buildings may ultimately be converted to other uses. We use 30% as a rough benchmark for the option value to covert to other uses. A fuller consideration of this option—which will be affected by interest rates, costs of conversion, and demand for other uses among other factors—is outside of the scope of our analysis, which is focused on valuing cash flows resulting from buildings operated as commercial office buildings. Gupta et al. (2023) studies conversions from office to residential in detail.

Figure G4: Robustness Tests for San Francisco

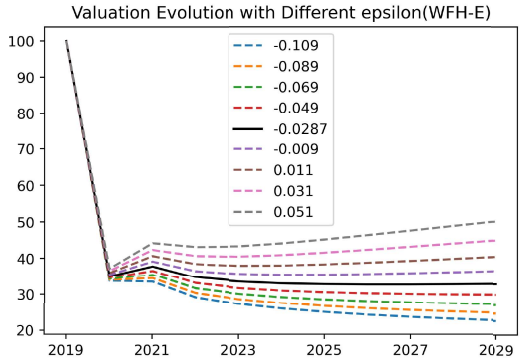

(a) Different $\epsilon(WFH - E)$

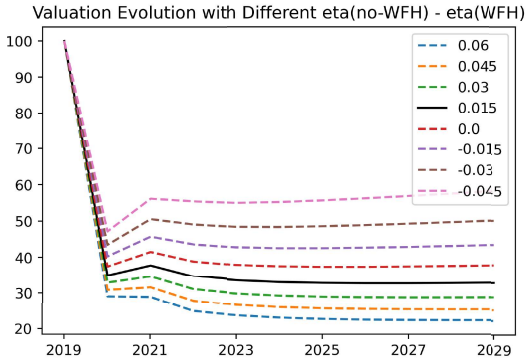

(b) Different $\eta(no - WFH) - \eta(WFH)$

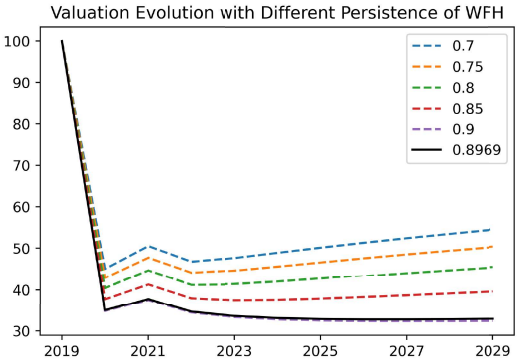

(c) Different Persistence of WFH

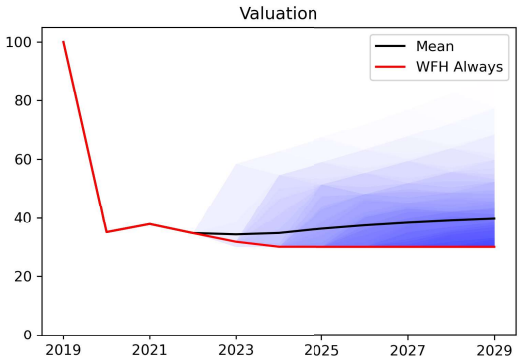

(d) Valuation $\geq$ 30% of Pre-pandemic Valuation